

Temporal Changes in the Observed Relationship between Cloud Cover and Surface Air Temperature

BOMIN SUN

Department of Geosciences, University of Massachusetts, Amherst, Amherst, Massachusetts

PAVEL YA. GROISMAN

National Climatic Data Center, Asheville, North Carolina

RAYMOND S. BRADLEY AND FRANK T. KEIMIG

Department of Geosciences, University of Massachusetts, Amherst, Amherst, Massachusetts

(Manuscript received 26 July 1999, in final form 28 December 1999)

ABSTRACT

The relationship between cloud cover and near-surface air temperature and its decadal changes are examined using the hourly synoptic data for the past four to six decades from five regions of the Northern Hemisphere: Canada, the United States, the former Soviet Union, China, and tropical islands of the western Pacific. The authors define the normalized cloud cover–surface air temperature relationship, NOCET or dT/dCL , as a temperature anomaly with a unit (one-tenth) deviation of total cloud cover from its average value. Then mean monthly NOCET time series (night- and daytime, separately) are area-averaged and parameterized as functions of surface air humidity and snow cover. The day- and nighttime NOCET variations are strongly anticorrelated with changes in surface humidity. Furthermore, the daytime NOCET changes are positively correlated to changes in snow cover extent. The regionally averaged nighttime NOCET varies from $-0.05 \text{ K tenth}^{-1}$ in the wet Tropics to 1.0 K tenth^{-1} at midlatitudes in winter. The daytime regional NOCET ranges from $-0.4 \text{ K tenth}^{-1}$ in the Tropics to 0.7 K tenth^{-1} at midlatitudes in winter.

The authors found a general strengthening of a daytime surface cooling during the post–World War II period associated with cloud cover over the United States and China, but a minor reduction of this cooling in higher latitudes. Furthermore, since the 1970s, a prominent increase in atmospheric humidity has significantly weakened the effectiveness of the surface warming (best seen at nighttime) associated with cloud cover.

The authors apportion the spatiotemporal field of interactions between total cloud cover and surface air temperature into a bivariate relationship (described by two equations, one for daytime and one for nighttime) with surface air humidity and snow cover and two constant factors. These factors are invariant in space and time domains. It is speculated that they may represent empirical estimates of the overall cloud cover effect on the surface air temperature.

1. Introduction

Clouds exert a dominant influence on the energy balance of the earth's climate through the cooling effect of albedo and the greenhouse warming effect. The interaction of clouds with radiation alters the surface–atmosphere heating distribution, which in turn drives atmospheric motion that is responsible for the redistribution of clouds. Due to the complexity of the multiscale nature of cloud formation and cloud–radiation interactions, the details of the interaction of cloudiness with

the state of the climate system remain unclear and constitute one of the major uncertainties in climate modeling and prediction (Cess et al. 1996; Weare et al. 1996). For instance, an intercomparison of general circulation models (GCMs) participating in the Atmospheric Model Intercomparison Project (AMIP-1) indicated that approximately one-third of the 30 GCMs show positive interannual correlation between total cloud cover and surface air temperature over the Northern Hemisphere land areas, while the others show a negative correlation (Mokhov and Love 1995). The large uncertainties of parameterizations representing cloud processes and cloud properties in climate models indicate that observations are critical for a better understanding of the role of cloudiness in present, past, and future climate variations.

Corresponding author address: Pavel Ya. Groisman, UCAR Project Scientist, National Climatic Data Center, Federal Building, 151 Patton Ave., Asheville, NC 28801.
E-mail: pgroisma@ncdc.noaa.gov

Recent field experiments (Barkstrom 1984; Rossow and Schiffer 1991; Stokes and Schwartz 1994; Wielicki et al. 1995) have provided detailed information on cloud properties and atmospheric radiative fluxes, thus making important contributions to our understanding of the processes that lead to changes in cloudiness. However, field data products are too short in time for long-term cloud–climate interaction studies. Also, most studies regarding the cloud–climate relationship focused on ocean areas (e.g., Weare 1994; Weaver and Ramanathan 1997; Norris 2000), where the climate regime and cloud properties are different from those over land areas (Kiehl 1994). The conventional surface-based observing network provides a unique opportunity to explore the large-scale spatial and temporal cloud–climate relationship over the earth’s land areas.

An approach, overall cloud effect, (OCE), has been developed by Groisman et al. (1996, 2000) to study the relation of total cloud cover (CL)¹ to surface air temperature (T), atmospheric pressure, wind, and humidity characteristics over the Northern Hemisphere land areas. The overall cloud effect on T is defined as

$$\text{OCET} = E(T) - E(T|\text{under clear-sky conditions}), \quad (1.1)$$

and/or

$$\text{OCET}_1 = E(T|\text{under overcast conditions}) - E(T), \quad (1.2)$$

where $E(\cdot)$ and $E(\cdot|\cdot)$ are mathematical expectation and conditional mathematical expectation, respectively. Despite the name, the statistics in Eqs. (1.1) and (1.2) do not represent causal relationships or forcings but are bivariate associations between CL and T . This noncausal OCET is driven by, in addition to cloud processes, many other physical processes that modify CL and T .

Based on synoptic surface data for the past several decades, Groisman et al. (1996, 2000) analyzed the long-term mean relationship between CL and T over land areas of the Northern Hemisphere. They found that surface air temperature variations associated with cloud cover exhibit strong seasonal and diurnal cycles, and vary with different geographical locations and climate regimes. Recent observational studies revealed that significant changes in surface air temperature (Vinnikov et al. 1990; Jones 1994; Houghton et al. 1996; Serreze et al. 2000), total cloudiness (cloud type) (Angell 1990; Henderson-Sellers 1992; Kaiser 1998; Sun and Groisman 2000), and tropospheric precipitable water (Ross

and Elliott 1996; Zhai and Eskridge 1997) have occurred in many land areas during the past several decades. So, these climate changes may cause changes in OCET. One of the purposes of this paper is to investigate the temporal changes in the CL– T relationship.

Clouds are an internal component of the climate system. The presence and variations of cloud sky coverage and cloud radiative effects are closely related to atmospheric humidity (Fung et al. 1984; Zhang et al. 1995; Sun and Groisman 1999; Groisman et al. 2000) and snow on the ground (Cess et al. 1991). Our second objective is to parameterize the CL– T relationship as functions of atmospheric humidity and snow cover. We expected that, after humidity and snow cover contributions are parameterized and removed, the residual terms of the CL– T relationship would show some spatial and/or temporal structure. But instead, our analysis of these residuals reveals only a kernel property of the CL– T relationship: two invariant constants (for nighttime and daytime, respectively) are present in each region, season, decade, and set of climate conditions, and our parameterization thus “describes” the entire spatial and temporal variability of this relationship.

The outline of this paper is as follows. The next section describes the data used in this study and its processing. Normalized OCET (NOCET) or an estimate of the derivative dT/dCL , defined as a temperature anomaly with a unit (one-tenth) deviation of cloud cover from its average value, is introduced in this section to better characterize the temporal CL– T relationship. Section 3 discusses and quantifies the parameterization of NOCET as a function of humidity and snow cover for nighttime and daytime separately. A general OCET model, represented by cloud cover, surface humidity, and snow cover, which is applicable to any time and any geographical land location, is constructed in this section. Trends in NOCET (OCET) in the past several decades in four regions of the Northern Hemisphere [the United States, Canada, the former Soviet Union (FUSSR), and China] are analyzed in section 4.

2. Data description and preprocessing

In this work, the Northern Hemisphere synoptic station dataset, described in Groisman et al. (1996, 2000), is used to conduct the study on the cloud cover–surface air temperature relationship, and its associations with atmospheric water vapor² and snow cover over the contiguous United States, southern Canada (south of 55°N), the southern area of the FUSSR (south of 60°N), eastern China (east of 110°E), and the western tropical Pacific

¹ Cloud cover is only one of many characteristics of cloudiness. However, sufficiently long time series with information about other cloudiness characteristics available from national archives are scant, and the definitions of these characteristics vary with time and by country. Therefore, we were not able to secure sufficient coverage for other cloudiness characteristics for our analyses, and throughout this paper we use only total cloud cover.

² Near-surface specific atmospheric humidity, q , was selected to characterize variations of lower tropospheric water vapor. This variable is always available at the same locations as T in our dataset and correlates reasonably well with the lower tropospheric water vapor content (Gandin et al. 1976).

TABLE 1. Major characteristics of the synoptic dataset used in this study.

Region	Number of stations	Periods of observations	Time increment
Contiguous United States	195	1948–93	Hourly
Canada (south of 55°N)	33	1954–93	Hourly
FUSSR (south of 60°N)	156	1936–90	3-hourly/6-hourly
China (east of 110°E)	101	1954–90	6-hourly
Western Pacific Tropics	9	1952–96	Hourly/3-hourly

(only the stations from the U.S. possessions and air bases are selected in this region). The hourly station data for North America cover the period from around the 1950s to 1993. The Chinese data are from 1954 to 1990 with a 6-hourly time increment. The FUSSR data cover the period from 1936 to 1990 with 6-hourly (before 1966) and 3-hourly (after 1966) measurements. Hourly and 3-hourly measurements at nine stations in the western tropical Pacific cover the period from the early 1950s to 1996. While assessing the CL– T relationship in nighttime (daytime) periods, we select five measurements at local standard time 2300, 2400, 0100, 0200, and 0300, (1200, 1300, 1400, 1500, and 1600) in North America and the western tropical Pacific, one measurement at 0200 (1400) LST in China, and one at 0100 (1300) LST or two (after 1966) at around noon (midnight), and 0300 (1500) LST in the FUSSR. Table 1 summarizes this information. The National Oceanic and Atmospheric Administration (NOAA) satellite-derived snow cover extent data (Matson and Wiesnet 1981; Robinson et al. 1993; Groisman et al. 1994b) are used in our analyses of the daytime CL– T relationship. The snow data span the period from 1972 to 1998, but we use only the data up to 1990, because we do not have the in situ synoptic observations over the FUSSR after that time.

In order to better understand the OCET changes in spatial and temporal domains and the associations of other climatic variables with OCET, we normalize OCET in Eqs. (1.1) and (1.2) by the amount that cloud cover differs (ΔCL) between average and clear-sky conditions, or between average and overcast conditions in a given period of time, t :

$$\text{NOCET}(t) = \text{OCET}(t)/\Delta CL(t) \quad \text{and} \quad (2.1)$$

$$\text{NOCET}_1(t) = \text{OCET}_1(t)/\Delta CL(t). \quad (2.2)$$

Thus, these two equations represent the estimates of the derivatives from the left (2.1) and from the right (2.2) of the surface air temperature with respect to total cloud cover.

In our study OCET is defined as the difference in surface air temperature between average and clear-sky (cloudiness $\leq 1/8$) conditions. In each year, for a given time of day, the mean monthly OCET is calculated by subtracting monthly mean surface air temperature under clear-sky conditions from mean temperature. Then, these temperature differences are averaged over the selected nighttime (daytime) period. Thus, time series of

monthly OCET are constructed for both nighttime and daytime at each station. Time series of the normalized CL– T relationship (NOCET) is then created by dividing OCET by the difference between monthly cloud amount with average conditions and with clear-sky conditions at each location. In a humid atmosphere, the lack of a sufficient number of clear-sky cases in a given month affects our ability to reliably estimate OCET. To ensure that our OCET assessment over North America and Eurasia is robust, and to secure reliable OCET estimates in the Tropics, where the clear-sky observations are scarce, we use the same approach to construct the normalized OCET₁ and NOCET₁ time series (where the sky coverage of overcast $\geq 7/8$) at each station. The comparison (appendix A) of NOCET₁ with NOCET indicates that there are no significant differences in these two OCET definitions, except the convenience of using a larger sample. However, this quasi linearity should not be taken for granted, because of the complexity of overcast situations, which can include *cumulus* and/or *stratus* clouds, as well as other types of clouds.

Sun and Groisman (1999) and Groisman et al. (1996, 2000) used 20–50 yr of hourly, 3-hourly, and 6-hourly observations to produce the climatological OCE estimates. The long time series provided statistically significant sample points for estimating long-term OCE. Now, working with the data and OCE estimates in individual months (i.e., with small sample sizes), we have to suppress the weather noise in order to get meaningful OCE. Area averaging can serve this purpose. Therefore, all OCET estimates, as well as other climate variables, such as mean monthly cloud amount (CL), surface air temperature (T), and specific humidity (q) under average, clear-sky, and overcast conditions are spatially averaged across the contiguous United States, southern Canada, the southern FUSSR, and eastern China by using the Thiessen polygon method (Thiessen 1911). To estimate the area-averaged variables in the western tropical Pacific, arithmetic averaging of the individual station data is used.

Finally, the countrywide averaged mean monthly time series of day- and nighttime OCET, OCET₁, NOCET, NOCET₁, CL, T , T_{clear} , T_{overcast} , q , q_{clear} , and q_{overcast} are produced and used in various statistical analyses described in the next section.

Several experiments have been conducted to test the robustness of our approach and are described in appendix A. A statistical method, the method of instrumental

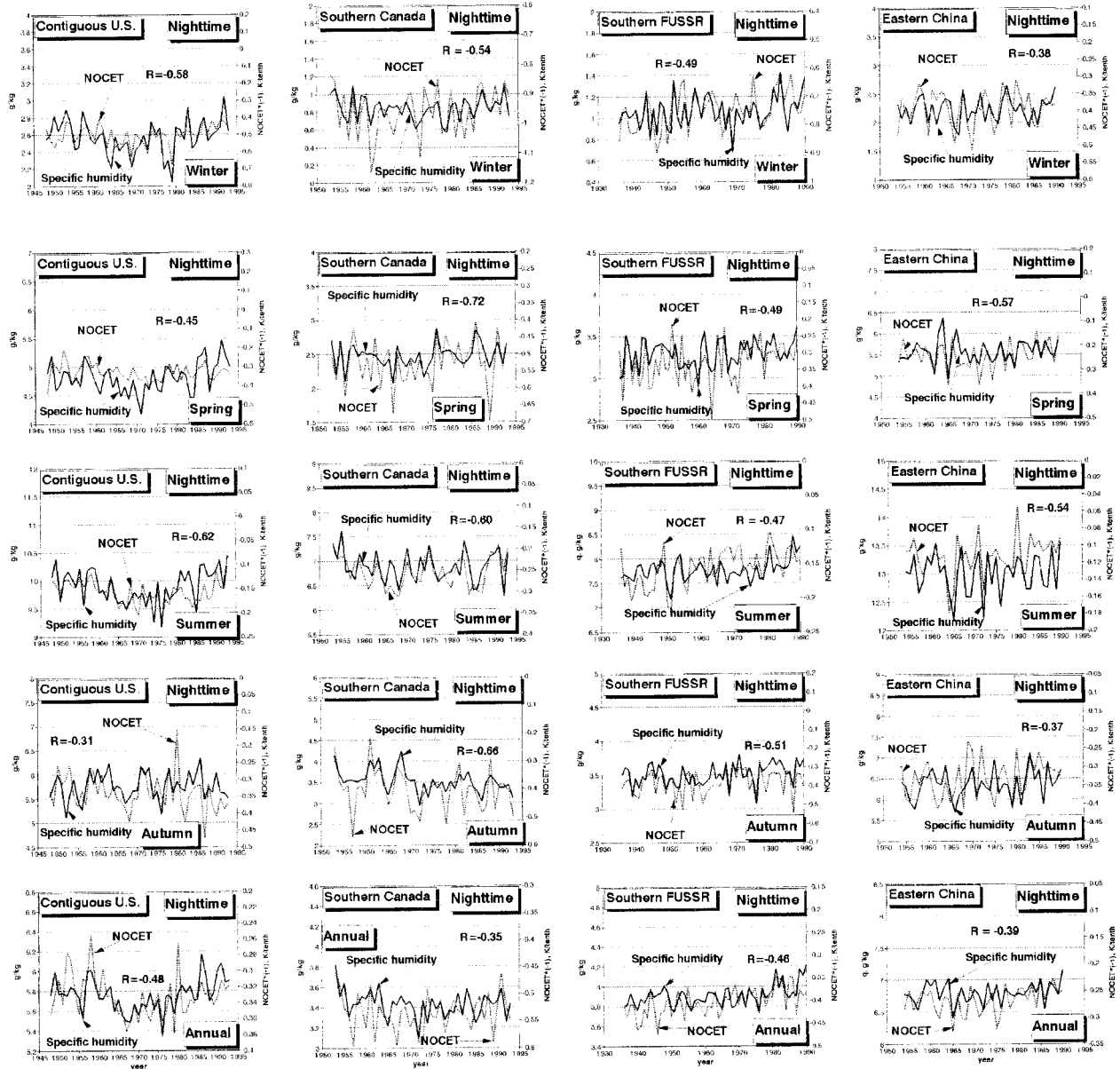


FIG. 1. Variations of mean seasonal/annual nighttime specific humidity under clear skies and the normalized cloud cover–surface air temperature relationship (NOCET) (multiplied by -1), area-averaged over the contiguous United States, southern Canada (south of 55°N), the FUSSR (south of 60°N), and eastern China (east of 110°E) (nighttime). Please note different scales of the y axes. Correlation coefficients, R , are statistically significant at the 0.05 level.

variable, employed throughout this paper is presented in appendix B. This method has not been used very often in climatic studies but is widely used in economics (Geary 1949; Kendall and Stuart 1967; Fisk 1967).

3. Parameterization of cloud cover–surface air temperature by surface air humidity and snow cover variations

a. Nighttime

Figure 1 shows the countrywide variations of the seasonal/annual NOCET (multiplied by -1) and mean sur-

face specific humidity under clear-sky conditions, q_{clear} . The statistically significant anticorrelation between NOCET and q_{clear} in each season and area (except in autumn over eastern China, which will be discussed later in this section) strongly indicates that changes in the nighttime NOCET are inversely associated with surface humidity. This conclusion is also supported by the fact (somewhat disguised in Fig. 1 by different y-axis scales) that over all regions of interest the winter NOCET is always larger than the summer NOCET.

Nighttime surface temperature change is closely correlated to surface downward longwave radiation change

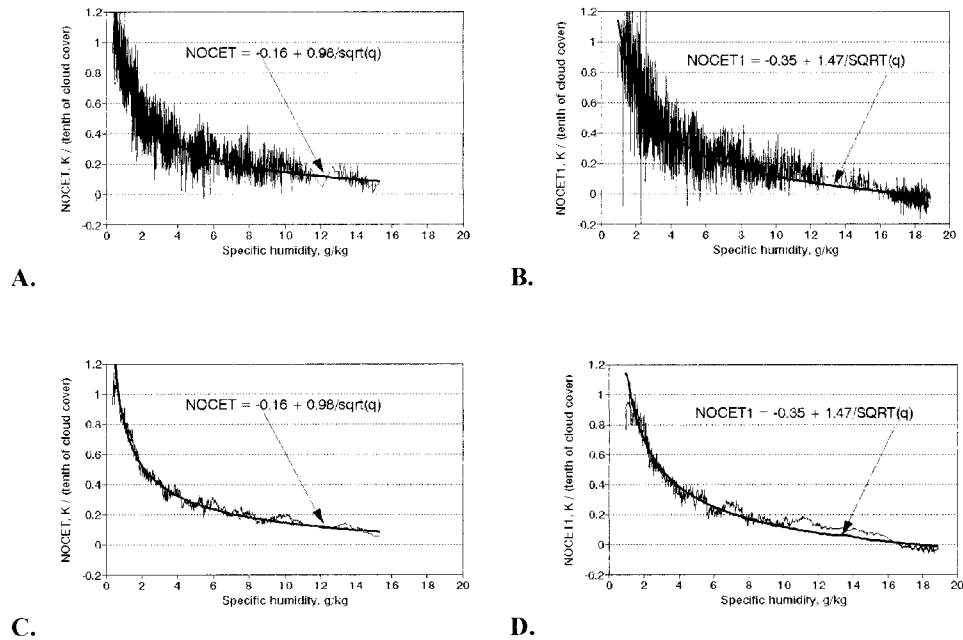


FIG. 2. The normalized nighttime CL– T relationship as a function of specific humidity and its functional approximation. (a) Estimates are based on 2148 individual monthly NOCET values area-averaged over the contiguous United States, Canada (south of 55°N), the FUSSR (south of 60°N), and China (east of 110°E). (b) Estimates are based on 2688 individual monthly NOCET₁ values area-averaged over the contiguous United States, Canada (south of 55°N), the FUSSR (south of 60°N), China (east of 110°E), and the western Pacific Tropics. (c) and (d) The same as (a) and (b), respectively, but a 20-point running averaging was applied to these estimates.

(Dai et al. 1999), which is directly related to low tropospheric humidity and temperature, in addition to the presence of cloud cover. Because of the strong coherence between low tropospheric and near-surface humidity (Gandin et al. 1976), the anticorrelation between q and NOCET in Fig. 1 also reflects the relationship between low tropospheric water vapor and clouds in affecting surface air temperature, as revealed by satellite observations (Stephens et al. 1994; Zhang et al. 1995). Low tropospheric and surface temperature affects NOCET and, therefore, the q –NOCET relationship through downward and upward longwave radiation. Our estimates (appendix A) indicate that the contribution of surface temperature variability is insignificant to the NOCET– q correlation. However, the NOCET– q correlation does indeed become better in winter and spring after the year-to-year temperature variability is suppressed.

Based on all the data points in Fig. 1, the functional relationship of NOCET with q_{clear} is approximated by the formula

$$\text{NOCET} = f(q_{\text{clear}}) = -0.14 + 0.93(q_{\text{clear}})^{-0.5}, \quad (3.1)$$

where the constant -0.5 is selected to mimic the contribution of near-surface air humidity to the downward

longwave radiation in the Brunt formula (Brunt 1932),³ q is measured in grams per kilogram, and the coefficients have been estimated by the least squares method. The least squares method gives biased estimates of the parameters of the linear functional relationship $Y = \alpha_0 + \alpha_1 X$, when the X variable is measured with error. Usually the absolute values of the α_i estimates are reduced (Kendall and Stuart 1967). Therefore, after the form of $f(q_{\text{clear}})$ is selected, we debias these parameters by applying the instrumental variable method (Geary 1949) and using the mean daytime solar elevation angle as this variable. The unbiased estimate of α_1 appears to be only 5% higher than that obtained by the least squares method, and Eq. (3.1) is converted to

$$\begin{aligned} \text{NOCET} &= f(q_{\text{clear}}) = \alpha_0 + \alpha_1(q_{\text{clear}})^{-0.5} \\ &= -0.16 + 0.98(q_{\text{clear}})^{-0.5}. \end{aligned} \quad (3.2)$$

Figure 2a shows the functional relationship of NOCET with q_{clear} (all the data points come from Fig. 1) and the goodness of fit of Eq. (3.2) with NOCET. The $f(q_{\text{clear}})$ in Eq. (3.2) describes 83% of the monthly countrywide NOCET variance. It is clear from Fig. 2a that the an-

³ We varied the power constant in Eq. (3.2) within broad limits and found that the best fit could be achieved when it is in the range of -0.4 to -0.6 .

TABLE 2. Goodness of fit of the nighttime NOCET parameterization with Eq. (3.2), by country. Here σ_{NOCET} is the standard deviation of monthly normalized cloud effect on surface air temperature averaged over the country; σ_{RT} is the standard deviation of the residual term of NOCET, RT, after the contribution of humidity variations has been subtracted; R^2 is the multiple correlation coefficient of NOCET and its approximation as a function of specific humidity under clear skies.

Variable/Country	United States	Canada	Former USSR	China
Bias, K tenth ⁻¹	0.04	0.02	-0.05	-0.01
σ_{NOCET} , K tenth ⁻¹	0.15	0.32	0.26	0.14
σ_{RT} , K tenth ⁻¹	0.08	0.12	0.09	0.10
R^2	0.75	0.87	0.87	0.45

tirelationship between q and NOCET is nonlinear; NOCET is more sensitive to changes in T in a dry atmosphere than in a humid atmosphere. For example, an additional 10% increase in total cloud cover corresponds to an increase in nighttime surface air temperature of 1 K in a dry atmosphere with monthly $q_{\text{clear}} \sim 0.8 \text{ g kg}^{-1}$, but of only 0.1 K in a humid atmosphere with $q_{\text{clear}} \sim 14 \text{ g kg}^{-1}$. Table 2 shows the goodness of fit of $f(q_{\text{clear}})$ in Eq. (3.2) with NOCET in each country we analyzed; it describes from 45% (China) to 87% (FUSSR and Canada) variance of monthly countrywide averaged nighttime NOCET variability, including the seasonal cycle.

Figure 2b depicts the statistical relationship between NOCET₁ and overcast surface specific humidity q_{overcast} . In this figure, the monthly NOCET₁ and q_{overcast} from the western tropical Pacific (represented by the last cluster of points with q values from ~ 17 to 19 g kg^{-1}) are included together with those values from the four countries. Figure 2b supports all of the conclusions derived from Fig. 2a and also gives us an alternative set of parameterizations for a humid atmosphere:

$$\text{NOCET}_1 = f(q_{\text{overcast}}) = -0.35 + 1.47(q_{\text{overcast}})^{-0.5}, \quad (3.3)$$

where q is measured in grams per kilogram. The debiasing estimate technique increases $f(q_{\text{overcast}})$ by only 5%, and these relationships again describe 83% of the monthly NOCET₁ variance. When we express NOCET₁ as a function of q_{clear} , an equation,

$$\text{NOCET}_1 = -0.20 + 0.98(q_{\text{clear}})^{-0.5}, \quad (3.4)$$

that describes 85% of the monthly NOCET₁ variance emerges [note the similarity with (3.2)]. All of these estimates have been performed using large samples, 2148 for NOCET and 2688 for NOCET₁ parameterizations,⁴ and random errors in these estimates are negligible.

Equation (3.3) provides an important x -axis exten-

⁴ To estimate parameters in Eqs. (3.2) and (3.4), a 2148 sample size has been used because we cannot accurately estimate q_{clear} in the western tropical Pacific due to sampling problems.

sion: for q_{overcast} above 16 g kg^{-1} the NOCET₁ estimates are close to zero or are negative. This indicates that clouds totally lose their longwave radiation warming effects in a humid atmosphere. So, the nighttime surface cooling associated with overcast in the humid Tropics in Fig. 2b may be caused by certain factors or processes, which do not interfere with the cloud longwave radiation effect, but directly affect the surface air temperature and are associated with cloud cover. These can be stronger surface winds, which contribute to a greater loss of surface energy (Jones et al. 1998; Shinoda et al. 1998; Groisman et al. 1996), more precipitation (Gosnell et al. 1995), and a residual inertia-driven result of the daytime surface and low tropospheric cooling associated with the presence of cloud cover. We believe that these factors/processes also operate over the extratropics,⁵ but they are more visible in a humid atmosphere, where the atmospheric water vapor below the cloud base masks the downward longwave radiation effects of clouds. Although synoptic atmospheric advection and other non-longwave radiation related factors and processes contribute to nighttime NOCET, their effect on nighttime NOCET appears to be rather small on the spatial and temporal scales used in our analysis. Thus, a significant portion of the nighttime CL- T relationship is well represented by the surface air humidity term in Eqs. (3.2) and (3.4), that is, $0.98(q_{\text{clear}})^{-0.5}$.

b. Daytime

The daytime NOCET is the CL- T relationship, to which both long- and shortwave effects of cloudiness contribute. Figure 3 shows an example of the similarity between the nighttime and daytime NOCET- q relationship: over the contiguous United States during summer the correlation coefficient between nighttime NOCET and q_{clear} is -0.62 , which is close to the daytime value of -0.45 . However, a rigorous method of checking whether the nighttime NOCET- q relationship can be used to account for the longwave effect of cloudiness and its relationship with surface air temperature in the daytime NOCET, is used to see whether the derivatives, $d\text{NOCET}/dq$, are the same (or statistically insignificantly different) between daytime and nighttime. Table 3 provides a proof that this is the case. Each line of this table gives two estimates of $d\text{NOCET}/dq_{\text{clear}}$ for nighttime and daytime, respectively. Each of these derivatives has been estimated using simple linear regression equations that approximate the general relationship between

⁵ For example, strong and frequent synoptic monsoonal advection over China during the cold season (Ding 1994) may affect surface air temperature associated with cloudiness, thus contaminating the q -NOCET relationship, and lowering their correlation (see Fig. 1). In spring and summer the advection process is less prominent, and, coincidentally, in these two seasons in each country under consideration, more than 23% (and up to 56% in spring in southern Canada) of the interannual NOCET variance is ascribed to q .

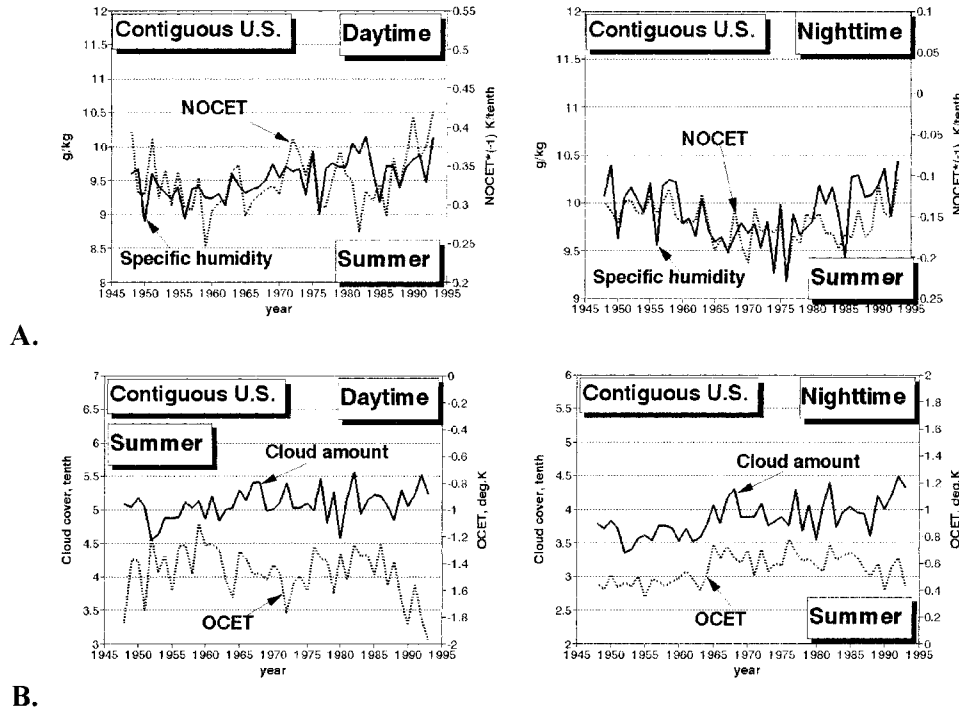


FIG. 3. Variations of mean summer (a) specific humidity under clear skies and NOCET (multiplied by -1) and (b) total cloud cover and OCET area-averaged over the contiguous United States.

NOCET and q_{clear} for a given season and country. In each case (except the regions where the daytime relationship between NOCET and q_{clear} is not seen at all) the hypothesis that these two derivatives are the same cannot be rejected at the 0.05 level of statistical significance. This exercise ensures us that we can use the parameterizations of the nighttime CL– T relationship to separate the shortwave component of the CL– T relationship from the daytime NOCET (i.e., simply subtract

the component responsible for the nighttime CL– T relationship and analyze the residual terms).

The shortwave radiation effects of cloud cover on surface air temperature are strongly related to cloud albedo, which is usually higher than that of the underlying surface (Hartmann 1994), and to a multiple reflection, which is when clouds reflect a part of the upward radiation back to the surface (Houze 1993). Also, a change in land surface characteristics, such as vegeta-

TABLE 3. Estimates of derivative $d\text{NOCET}/dq_{\text{clear}}$ for night- and daytime over four different countries and seasons.

County	Season	Nighttime estimates		Daytime estimates	
		$d\text{NOCET}/dq_{\text{clear}}$	Its σ	$d\text{NOCET}/dq_{\text{clear}}$	Its σ
Contiguous United States	Winter	-0.163	0.035	-0.153	0.052
	Spring	-0.077	0.022	-0.069	0.034
	Summer	-0.051	0.010	-0.058	0.017
	Autumn	-0.062	0.029	-0.077	0.032
Canada (south of 55°N)	Winter	-0.317	0.079	-0.354	0.073
	Spring	-0.266	0.041	-0.226	0.053
	Summer	-0.068	0.015	-0.060	0.024
	Autumn	-0.176	0.032	-0.235	0.039
FUSSR (south of 60°N)	Winter	-0.220	0.054	-0.223	0.048
	Spring	-0.180	0.044	-0.203	0.035
	Summer	-0.054	0.014	-0.011*	0.021
	Autumn	-0.203	0.048	-0.118*	0.044
China (east of 110°E)	Winter	-0.091	0.038	-0.034*	0.027
	Spring	-0.117	0.028	-0.005*	0.022
	Summer	-0.034	0.009	-0.024	0.012
	Autumn	-0.057	0.024	-0.029*	0.025

* This regression estimate is not statistically significantly different from zero.

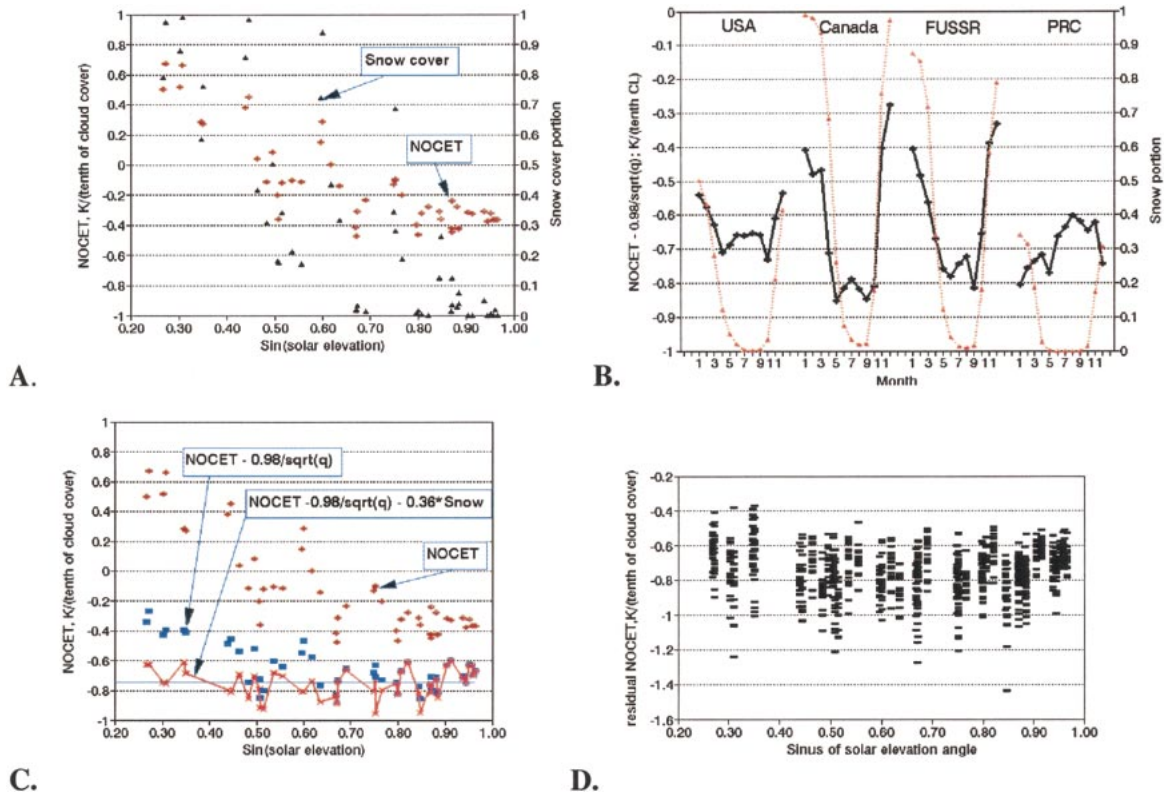


FIG. 4. Daytime normalized cloud cover–surface air temperature relationship (long-term monthly mean values) and its decomposition. (a) NOCET and snow cover as a function of the average mean daytime monthly solar elevation, φ . Each point represents a countrywide mean monthly value of NOCET and snow cover for the contiguous United States, southern Canada (south of 55°N), the FUSSR (south of 60°N), and eastern China (east of 110°E). (b) Residual term of the NOCET after removal of the q contribution, RT_1 (solid lines), and mean monthly snow cover for four countries (dotted lines). (c) NOCET and its residual terms after the contributions of humidity and snow cover have been accounted for. Plotted vs $\sin(\varphi)$, the final residual term (solid line) shows no significant correlation with solar elevation. (d) Residual term, RT_2 , for individual months during the period of 1972–90, plotted vs $\sin(\varphi)$.

tion, soil moisture, and snow cover, can affect surface air temperature, and therefore daytime NOCET, through a change in atmosphere–surface heat flux exchange, and more importantly, through a change in surface albedo. The snow cover factor is the most effective in changing surface albedo, and therefore surface temperature, in the seasonal cycle; surface albedo can increase quickly from ~ 0.2 for bare soil to ~ 0.8 for a freshly fallen snow on the ground (Henderson-Sellers and Robinson 1986). We do not have any large-scale representative soil moisture data for the four countries under consideration and leave the effects of vegetation (and its related effects in evapotranspiration) to our future study. But snow on the ground is a first-order factor that should be taken into account. Another essential first-order factor is the amount of solar radiation available at the top of the atmosphere, which can be reflected by clouds and thus affects the geographical distribution and temporal variation of daytime NOCET. Figure 4a presents a correlation graph of daytime NOCET and snow cover versus the sine of mean monthly midday solar elevation over each of the four countries. This elevation changes from

15° in December over the FUSSR south of 60°N to 75° in June over eastern China. The mean monthly portion of the country with snow on the ground during the period from 1972 to 1992 from NOAA satellite imagery (Matson and Wiesnet 1981; Robinson et al. 1993) characterizes snow climatology in this graph.⁶ This correlation graph illustrates how the daytime NOCET chang-

⁶ There are two reservations related to the use of satellite-derived snow cover in our analyses. First, we use here an averaging period (1972–92) that is significantly different from the periods used for the long-term mean NOCET estimates. An assessment of the same period (common for all time series) has shown that the different periods do not affect the results discussed in this section. The second problem is more serious. While the satellite-derived snow cover extent provides the best spatial coverage, the “countrywide” NOCET estimates are based only on the first-order stations, airports. In the western United States and Canada, and in the eastern FUSSR and China, these stations are located, on average, at lower elevations than the general terrain. This becomes most visible in late summer, when snow cover extent is not zero over the United States, Canada, and the FUSSR, but all stations in these three countries do not have snow on the ground and, thus, cannot report its effect on NOCET.

es with latitude and season; with low maximum solar elevations NOCET is positive, that is, cloud cover is associated with a higher surface air temperature, but with high solar elevations the daytime cooling associated with cloud cover prevails. After the longwave component of the CL– T relationship, represented by $0.98(q_{\text{clear}})^{-0.5}$, has been removed from the daytime NOCET, Fig. 4b shows that the residual term, RT_1 , is negative, and in the cold season is closely correlated with snow cover on the ground. The year-round multiple correlation coefficient R^2 , between RT_1 and snow cover extent S , for all four countries together is 0.60, and for three countries (except eastern China) is 0.70. Here it should be noted that it is not the snow cover extent itself but the snow albedo that is affecting NOCET. Snow aging reduces its albedo and thus increases the difference in shortwave radiation that the surface absorbs between cloudy and clear-sky conditions, therefore enhancing the surface air temperature difference between these two cases compared to the situation with new snow on the ground. Figure 4b illustrates this: in Canada and the FUSSR the December snow cover extent is close to that in February, but, on average, the upper layer of snow on the ground during the accumulation period is “fresher” than that at the end of the winter. As a result, we find the February RT_1 to be much less (negatively) than in December over these two countries. Only a small portion of eastern China has permanent snow cover during the winter. This and the valley locations of the airports make the relationship between snow cover and RT_1 insignificant over this country.

The regression of monthly RT_1 on S yields

$$RT_1 = 0.31S - 0.74$$

$$(R^2 = 0.36, \text{ with sample size } N = 912),$$

and the use of the same instrumental variable (solar elevation angle) increases the dRT_1/dS parameter to 0.35:

$$RT_1 = 0.35S - 0.75. \quad (3.5)$$

In this analysis we use the data only for the common period of all observations (meteorological and satellite snow cover): 1972–90. Regrettably, in this particular case, due to the artificial correlation between solar elevation (our instrumental variable ζ) and snow aging (which contributes to the error, δ , of the functional relationship between RT_1 and S), the condition $\text{cov}(\delta, \zeta) = 0$ is not achieved, and the parameters in (3.5) still can be somewhat biased.

Figure 4c shows the daytime long-term mean monthly NOCET estimates for four countries with gradually removed contributions of other factors; the squares show the RT_1 values, and the solid line depicts the residual term of NOCET, RT_2 , after the longwave component of the CL– T relationship represented by $0.98(q_{\text{clear}})^{-0.5}$ in Eq. (3.2) and the S effects represented by $0.35S$ in Eq. (3.5) are accounted for. Note that RT_2 is no longer cor-

related with the amount of incoming solar radiation. Its mean value is ~ -0.75 and its standard deviation is less than 0.1. The variance of RT_2 could be further reduced, if we had detailed snow cover information such as snow age, wetness, and color (Warren and Wiscombe 1980). Figure 4d shows that, after the effects of external forcing embedded into atmospheric humidity and snow cover variations have been taken into account, we do not need to further account for the insolation variability in NOCET.

c. General model of the cloud cover–surface air temperature relationship

We summarize our findings in this section. Using hourly data from several regions of the Northern Hemisphere, spread from high latitudes to the Tropics, we consequently decomposed the association of cloudiness with surface air temperature into the product of cloud cover, CL, and the normalized cloud cover–surface air temperature relationship, NOCET.⁷ The latter was then parameterized using two other internal climatic variables, specific humidity under clear skies, q_{clear} , and snow on the ground, S :

$$\begin{aligned} \text{NOCET}(\text{nighttime}) - 0.98(q_{\text{clear}})^{-0.5} + 0 \\ + 0.16 = \varepsilon_1 \quad \text{and} \end{aligned} \quad (3.6)$$

$$\begin{aligned} \text{NOCET}(\text{daytime}) - 0.98(q_{\text{clear}})^{-0.5} - 0.35S \\ + 0.75 = \varepsilon_2. \end{aligned} \quad (3.7)$$

Equations (3.6) and (3.7) can be interpreted as empirical estimates of the derivative dT/dCL from the left. Our analysis shows that the differences with the estimates of this derivative from the right are minimal [cf. Eqs. (3.2) and (3.4)]. A unit of cloud cover, after a corresponding contribution of changes in atmospheric humidity and snow on the ground are taken into account, is noticeably associated with a cooling of surface air by 0.16 K at nighttime and 0.75 K in daytime. The same cooling occurs in winter in high latitudes and in summer in the Tropics. We cannot attribute these universal constants to any specific forcing without physical modeling. They were found as a residual term (intercept) of statistical analyses described above. But it is essential to assume that the nighttime cooling is perhaps due to cold air advection, less stable stratification at nights with cloud cover compared to clear-sky nights (and thus a more intensive turbulent heat flux from surface to the atmosphere, and more precipitation), or a residual inertia-driven consequence of daytime processes. On the other hand, daytime cooling is mostly a *direct* effect of a higher cloud albedo compared to most surfaces, in addition to the contributions from those factors or pro-

⁷ The accuracy of this decomposition is discussed in appendix A.

TABLE 4. NOCET variance, D , and the variance of residual terms in Eqs. (3.6) and (3.7) ($K \text{ tenth}^{-1}$ of cloud cover)². The residual terms ε of the monthly country wide averaged NOCET estimates over the four countries are under consideration; $\bar{\varepsilon}$ are long-term time-averaged values of ε .

Period	$D(\text{NOCET})$	$D\varepsilon$	$D\bar{\varepsilon}$
Nighttime	0.06	0.01	0.004
Daytime	0.11	0.02	0.01

cesses occurring during nighttime. Whatever the nature of these factors, they represent our empirical estimates of the overall global cloud cover effect on the surface air temperature, dT/dCL , when the interaction with snow cover and/or atmospheric humidity has been accounted for or (as in the humid Tropics) is absent or weak.

The residual terms, ε , in our parameterizations in Eqs. (3.6) and (3.7) are rather small compared to NOCET variations (Table 4). It would be very interesting to find out if there is any additional (and unexplained) relationship that “organizes” the behavior of these terms. Therefore, we test the residual terms, RT (for nighttime) and RT_2 (for daytime), for each country in order to reveal some possible systematic trends that may hint at some additional factors that were not taken into account. Our analysis (not shown; cf. Sun and Groisman 1999) clearly indicated that there are no trends in these terms. Moreover, in each season over each region the mean values of ε in Eqs. (3.6) and (3.7) are close to 0. The random scatter of monthly RT and RT_2 characterizes a goodness of fit of our model for different countries. At nighttime the scatter is less than in the daytime, and in the northern countries (Canada, Russia) it is larger than in the United States and China. The more complete spatial coverage of the contiguous U.S. stations (Table 1) reduces the variance of the RT and RT_2 estimates in this country compared to others (Sun and Groisman 1999).

The $CL-T$ relationships are bivariate relationships between internal components of the climatic system that are not yet well understood. Groisman et al. (1996, 2000) quantified them using synoptic observational data in the hope that this quantification can be used to additionally test the ability of contemporary global climate models, GCMs, to reproduce contemporary climate variations. Below we continue this test and show how an experiment with a reliable GCM allows us to extend our judgment about the $CL-T$ relationship for changing climate conditions. Groisman et al. (2000) compared patterns of the long-term empirical OCET estimates with those patterns reproduced by several global climate models that participated in AMIP-1. They found that, while some of these models cannot reproduce the sign of the warm season OCET over the Northern Hemispheric land areas, others reasonably well reproduce sign, pattern, and absolute values of the $CL-T$ and $CL-q$ relationships. One of the latter GCMs was the Max

TABLE 5. Noncentered residual terms of NOCET over land areas after effects of humidity and snow cover are accounted for ($K \text{ tenth}^{-1}$ of total cloud cover). Empirical data (this study) and the model estimates from the time-slice Max Planck Institute high-resolution, T106, GCM experiments (Jul, snow-free land areas).

Time	This study	MPI	MPI
		(Control run)	($2 \times \text{CO}_2$ run)
Nighttime	-0.16	-0.31	-0.32
Daytime	-0.75	-0.76	-0.77

Planck Institute (Hamburg, Germany) model, ECHAM3. The performance of this GCM allows us to check the adequacy of the model’s own “invariants,” similar to RT and RT_2 , which we established in Eqs. (3.6) and (3.7) from the empirical data. We used several years of the control run generated in the time-slice experiment (Cubasch et al. 1995) by the high-resolution (T106) next-generation Max Planck Institute GCM, ECHAM4. The data for each grid cell (four times per day) for each month is processed in a similar manner as the empirical data we used. But we skipped the estimation step and ascribed the empirical values of $d\text{NOCET}/dq$ and $d\text{NOCET}/dS$ from Eqs. (3.2) and (3.5) to the model q and S components of the $CL-T$ relationship. Nevertheless, the ECHAM4 control run precisely reproduced the mean value of the daytime invariant in Eq. (3.7) and gave a value of the nighttime invariant of the same sign [also twice as large as in Eq. (3.6)] (Table 5). We applied the same procedure to the ECHAM4 perturbed climate experiment ($2 \times \text{CO}_2$) and found that the model mean values of these two invariants do not change. This experiment allows us to add to our conclusions that these day- and nighttime invariants of the $CL-T$ relationship do not change, not only geographically and temporally from seasons to decades, but also in large-scale climate change scenarios such as the $2 \times \text{CO}_2$ warm world.

4. Trends of temporal changes in the cloud cover-surface air temperature relationship

Figure 5 presents the annual countrywide averaged time series of daytime CL , q_{clear} , NOCET, and OCET for the period of records available to us. We observe a significant increase in total cloud cover over the contiguous United States and a significant decrease over eastern China. Over the FUSSR and Canada, annual total cloud cover changes are insignificant. We found a significant increase in near-surface clear-sky humidity over three of these regions, except southern Canada where q_{clear} decreased (Fig. 5) and strong east-west differences in climatic trends have been reported (Environment Canada 1995). These changes in CL and q_{clear} mostly define temporal changes in the daytime OCET and NOCET, especially when CL and q_{clear} effects act in the same direction (e.g., over the contiguous United States).

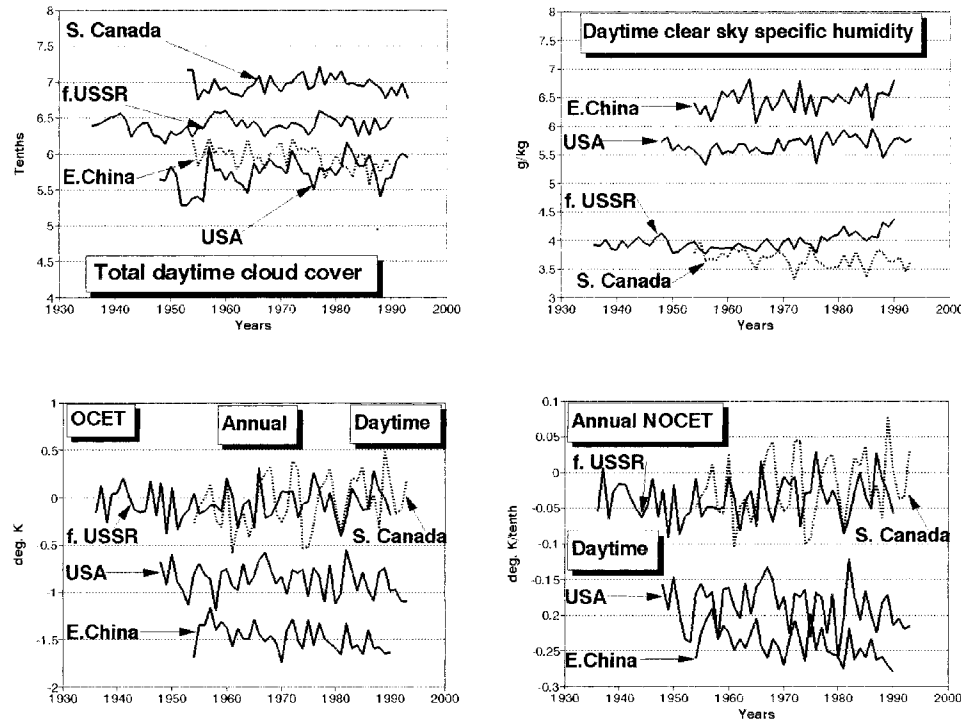


FIG. 5. Variations of mean annual daytime cloud cover, specific humidity under clear skies, OCET, and NOCET area-averaged over four regions: Canada (south of 55°N), the FUSSR (south of 60°N), the contiguous United States, and China (east of 110°E).

We observe in Fig. 5 a tendency for daytime OCET and NOCET to decrease over eastern China and the contiguous United States and to increase over southern Canada, with no change over the southern FUSSR during the post-World War II (WWII) period. This suggests that the portion of daytime surface cooling associated with cloud cover has become stronger in the subtropical land areas (from approximately 25° to 45°N), and somewhat weaker in the midlatitude land areas (from approximately 45° to 60°N). Over the midlatitude land areas, a significant retreat of snow cover has been documented for the post-WWII period (Groisman et al. 1994a,b; Meshcherskaya et al. 1995; Brown 1997). According to Eq. (3.7) this should exaggerate the cloud interaction with the surface temperatures by making daytime NOCET more negative, when it is negative. But, in Canada, this retreat was accompanied by decreases in humidity that opposed the cooling associated with snow cover retreat and thus reversed trends in OCET and NOCET.

Generally speaking, we do not find many significant changes in the nighttime NOCET over these four countries during the entire post-WWII period. However, Fig. 1 indicates that since the 1970s all four regions in almost all seasons, particularly in winter, present a decreasing trend in nighttime NOCET, suggesting that the nighttime surface warming associated with one unit of cloud cover has decreased.

Table 6 presents the long-term mean seasonal values

of countrywide averaged time series of CL, q_{clear} , NOCET, and OCET, and their linear trends (if they are statistically significant at least at the 0.10 level) for the period when the data are available for all four countries (1954–90). It summarizes the findings of this section. Finally, we focus on three regional aspects of the temporal CL– T relationship in the past several decades that deserve special attention and discussion.

a. Summer over the contiguous United States

Significant trends in U.S. cloud cover (especially in summer and autumn) have been reported by Plantico and Karl (1990) and later by Karl et al. (1993). These trends should be the major forcing behind the increase of the absolute OCET values; at night more warming and in daytime more cooling should be exhibited, both associated with the increased cloud cover. However, Fig. 3 suggests a nonlinearity in temporal OCET changes and shows why the trends in OCET can differ from those in cloud amount. In the contiguous United States, CL has been increasing from the 1950s to the 1990s, while OCET increased only from the mid-1950s to the early 1970s (and the increase in OCET is obviously more rapid than the increase in cloud amount), but afterward decreased somewhat. Our present analysis indicates that these differences in the interdecadal changes have been modulated by the decreased q from the mid-

TABLE 6. Mean values and trends in mean seasonal countrywide cloud cover (CL), specific humidity under clear skies (q_{clear}), normalized cloud effect on surface air temperature (NOCET), and overall cloud effect on surface air temperature (OCET), for the period from 1954 through 1990. (a) Nighttime and (b) daytime. Only statistically significant trends at the 0.05 level are presented.

Country	Season	CL		q_{clear}		NOCET		OCET	
		Tenth	% decade ⁻¹	g kg ⁻¹	% decade ⁻¹	K tenth ⁻¹	K yr ⁻¹	K	K decade ⁻¹
a. Nighttime									
Contiguous United States	Winter	5.4	—	2.5	—	0.5	—	2.7	—
	Spring	4.9	—	4.8	—	0.3	—	1.6	—
	Summer	3.9	2.6	9.9	—	0.2	—	0.6	0.04
	Autumn	4.3	3.6	5.8	—	0.3	—	1.4	0.08
Canada (south of 55°N)	Winter	6.0	—	0.8	—	1.0	—	5.3	—
	Spring	5.5	1.4	2.5	—	0.5	—	2.7	—
	Summer	5.3	—	6.9	—	0.3	—	1.2	—
	Autumn	6.4	—	3.5	-2.3	0.4	—	2.5	—
FUSSR (south of 60°N)	Winter	5.9	—	1.1	—	0.7	—	4.2	—
	Spring	5.1	—	3.3	2.1	0.3	-0.02	1.6	-0.10
	Summer	4.5	1.3	7.8	1.1	0.2	-0.01	0.6	—
	Autumn	5.4	—	3.5	1.5	0.4	—	2.1	—
China (east of 110°E)	Winter	4.1	—	2.2	—	0.4	—	1.3	—
	Spring	5.3	-2.5	5.6	—	0.2	—	0.9	—
	Summer	5.5	-2.1	13.0	—	0.1	—	0.6	—
	Autumn	4.4	—	6.4	—	0.3	—	1.2	-0.08
	Annual	4.8	-1.8	6.8	—	0.27	-0.01	1.0	-0.05
b. Daytime									
Contiguous United States	Winter	6.4	—	2.8	—	0.1	—	0.4	—
	Spring	6.2	—	4.6	2.2	-0.2	—	-1.2	—
	Summer	5.1	—	9.5	1.6	-0.3	-0.01	-1.4	-0.04*
	Autumn	5.4	2.5	5.7	—	-0.2	—	-1.2	—
Canada (south of 55°N)	Winter	6.9	—	1.0	—	0.6	—	3.6	—
	Spring	6.8	—	2.7	—	-0.1	—	-0.3	—
	Summer	6.8	—	7.1	—	-0.4	—	-2.4	—
	Autumn	7.4	—	3.9	-3.4	-0.2	0.04	-1.1	0.23*
FUSSR (south of 60°N)	Winter	6.6	—	1.2	—	0.5	—	3.0	—
	Spring	6.6	—	3.2	3.4	-0.1	—	-0.6	—
	Summer	5.9	—	7.8	2.6	-0.4	0.01*	-2.2	—
	Autumn	6.5	—	3.8	2.5	-0.1	—	-0.4	—
China (east of 110°E)	Winter	4.9	—	2.3	—	-0.1	—	-0.8	-0.09
	Spring	6.6	-1.2	5.2	—	-0.3	-0.02	-1.9	—
	Summer	6.9	-1.3	12.5	—	-0.4	—	-2.1	—
	Autumn	5.4	—	5.9	—	-0.2	—	-1.1	—
	Annual	6.0	-1.1	6.5	0.8*	-0.24	-0.01	-1.5	-0.06

* Estimate is statistically significant only at the 0.10 level.

1950s to the late 1970s (and associated with it increased NOCET) and the increase in q afterward.

b. Summer over the former USSR south of 60°N

In this region the most prominent feature of systematic changes during the period from 1950 to 1990 is a significant increase (of 1%–3% decade⁻¹) in mean monthly near-surface air humidity from April through September (Fig. 6, Table 6), which should lead to a decrease in nighttime NOCET. As a result, there are no trends in nighttime surface warming associated with cloud cover (i.e., an increase in nighttime OCET) during the past 40 years, in spite of a pronounced increasing trend in cloud amount. Also, in spring the surface specific humidity increase (of 2% decade⁻¹) has significantly reduced the nighttime OCET (by 0.1 K or by 6% decade⁻¹) over this country (Table 6).

c. Diurnal temperature range changes over China

An increase in total cloud cover has been suggested as one of the most important factors responsible for the observed decrease in the diurnal temperature range (DTR) (Karl et al. 1993; Hansen et al. 1995; Dai et al. 1999). In China, as in many other regions, the DTR has decreased in the past several decades, but total cloud cover has also decreased during the same period (Kaiser 1998). Table 6 and Figs. 1 and 5 clarify this. First of all, the long-term mean nighttime OCET over China is smaller, and daytime OCET is larger compared to the other three countries (Groisman et al. 1996, 2000; Table 6 and Figs. 5 and 1). Second, an increase in surface humidity [and an increase in atmospheric precipitable water (cf. Zhai and Escribde 1997)] led to a decrease in the nighttime NOCET, but the decrease in the daytime NOCET became even stronger due to an increase in q during the same period. So, the daytime changes in sur-

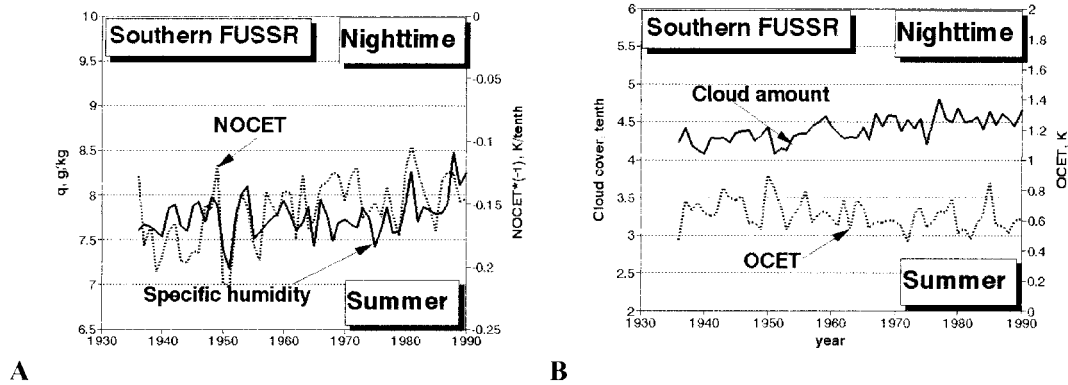


FIG. 6. Variations of mean summer nighttime (a) specific humidity under clear skies and NOCET (multiplied by -1) and (b) total cloud cover and OCET area-averaged over the FUSSR (south of 60°N).

face air temperature associated with cloud cover have thus been stronger than those at night and have nullified (or even reversed) the contribution of the cloud cover changes to the change in the DTR over eastern China.

5. Conclusions

We estimated empirically the full derivatives of near-surface air temperature with respect to total cloud cover, dT/dCL , over five regions of the Northern Hemisphere land areas: the contiguous United States, Canada, the former USSR, China, and western tropical Pacific islands. We named them normalized overall cloud effect and showed that its area-averaged monthly values (day- and nighttime, separately) can be easily parameterized as a function of two other internal variables, specific humidity and (in daytime only) snow cover fraction. Thus, we reduced the effects of total cloud cover, CL, on surface air temperature to a product of CL and a known function of two better known variables, near-surface humidity and snow cover, and traced their changes during the past 40–60 years. The most important among these changes were as follows.

- There was a general strengthening of a daytime surface cooling associated with cloud cover (in absolute values and per unit of cloud cover) over subtropical land areas (the United States and China) and a slight weakening of this cooling in higher latitudes.
- Since the 1970s, there has been a prominent increase in atmospheric humidity that significantly weakened the effectiveness of the surface warming associated with cloud cover (best seen at nighttime) over all four extratropical regions under consideration the United States, Canada, the former USSR, and China). We conclude that a direct longwave radiative interaction between clouds and surface air temperature has been gradually weakened during the past several decades due to this increase in atmospheric humidity.

After the contribution of bivariate relationships with snow cover and humidity was removed from the dT/dCL

data, we hoped to “discover” trends and/or manifestation of other forcings and/or feedbacks related to the interactions between total cloud cover and surface air temperature. Instead we found a very important thing: *nothing else*. The residuals of these bivariate relationships (two constants for night- and daytime, respectively) appeared to be invariants, which do not change geographically, seasonally, or interannually during the past several decades. We checked the behavior of these two residuals in a $2 \times \text{CO}_2$ experiment and found that they did not change there either. We speculate that these invariants represent the empirical estimates of the global overall cloud cover effect on the surface air temperature.

Changes in cloud cover–surface air temperature interactions, OCET, cannot be easily reduced to the effect of mean cloud amount increase/decrease. We even observe an OCET change opposite to that of cloud cover in sign (e.g., in China).

Acknowledgments. We thank Dr. Aiguo Dai (U.S. National Center for Atmospheric Research) and an anonymous reviewer for thoughtful comments and recommendations. NOAA Climate Change Data and Detection Program element of NOAA’s Office of Global Programs, NOAA National Climatic Data Center, National Science Foundation Grant ATM-9905399, and U.S. Department of Energy Grant DE-FG02-98ER626604 provided support for this study.

APPENDIX A

Several Technical Aspects of NOCET and OCET Estimation

a. Comparison of NOCET and NOCET₁ estimates

Monthly OCE at a station can be inaccurate if there are few clear-sky observations in a month of a year. This situation can occur over a humid area and/or during the wet season, and over some parts of high latitudes with daily cloud amount above 5 octas. Therefore, we assess the robustness of the cloud cover–surface air tem-

TABLE A1. Mean values, standard deviations, and correlations of NOCET and NOCET₁ nighttime estimates (K tenth⁻¹ of cloud cover). The NOCET estimates for the western tropical Pacific are not available due to a small sample size for clear-sky conditions in this area.

Region	Season	Mean value		Standard deviation		Correlation
		NOCET	NOCET ₁	NOCET	NOCET ₁	
Contiguous United States	Winter	0.501	0.472	0.056	0.058	0.94
	Spring	0.327	0.277	0.045	0.042	0.94
	Summer	0.157	0.118	0.024	0.025	0.89
	Autumn	0.339	0.293	0.055	0.055	0.97
Canada (south of 55°N)	Winter	0.959	0.960	0.078	0.074	0.88
	Spring	0.525	0.486	0.065	0.066	0.94
	Summer	0.254	0.205	0.035	0.039	0.81
	Autumn	0.402	0.379	0.073	0.075	0.93
FUSSR (south of 60°N)	Winter	0.746	0.744	0.066	0.065	0.92
	Spring	0.329	0.298	0.060	0.055	0.97
	Summer	0.155	0.118	0.026	0.027	0.88
	Autumn	0.382	0.341	0.064	0.064	0.79
China (east of 110°E)	Winter	0.392	0.381	0.052	0.051	0.96
	Spring	0.240	0.213	0.058	0.055	0.98
	Summer	0.113	0.089	0.023	0.025	0.95
	Autumn	0.331	0.310	0.053	0.053	0.97
Western Pacific Tropics	Winter		-0.016		0.026	N/A
	Spring		-0.031		0.023	N/A
	Summer		-0.045		0.024	N/A
	Autumn		-0.016		0.024	N/A

perature relationship by comparing the areally averaged NOCET with NOCET₁. This comparison can also provide a hint about possible nonlinearity in OCET. Table A1 shows mean values and the cross-correlation between NOCET and NOCET₁ over the contiguous United States, southern Canada, the southern FUSSR, and eastern China. All correlation coefficients in each country and season have passed the 1% significance *t* test, indicating that our estimates are quite reliable. While estimating the derivative dT/dCL from the left and from the right as $\Delta T/\Delta CL$, we could not make Δ infinitesimal, and Fig. 2 shows that humidity, which is generally higher when CL is between overcast and average than when CL is between clear skies and average, should make NOCET₁ less than NOCET. In summer the correlation between two NOCET estimates is lower than in other seasons, and the estimates of the derivative from the left, NOCET, are $\sim 30\%$ higher than those for the derivative from the right, NOCET₁ (Table A1). This can be due to a smaller number of clear-sky cases compared to other seasons, a stronger land surface heat flux exchange related to stronger convective processes, and precipitation generally associated with overcast conditions and, thus, with NOCET₁. Comparison of Eqs. (3.2) and (3.4) shows that the effect of this nonlinearity on our parameterization is minimal.

b. Effects of the accuracy of the nighttime cloud observations on our results

Hahn et al. (1995) have shown that the in situ measurements of nighttime average cloud cover (frequency of clear-sky occurrence) are usually underestimated (overestimated) due to inadequate illumination of the clouds. This could affect our estimates of nighttime

OCET and NOCET, which are based on surface observations without consideration of the nighttime detection bias in the cloud cover. Therefore, we checked the reliability of obtained CL–*T* relationship estimates by using the moonlight criterion suggested by Hahn et al. (1995).

Dr. C. J. Hahn (1998, personal communication) kindly provided us with a subroutine that was used in the determination of the questionable nighttime cloud observations (Hahn et al. 1995). The application of this illumination (moonlight) criterion discards about two-thirds of midnight cloud observations, and thus prevents us from computing the year-to-year NOCET and OCET time series. This situation is particularly serious in the FUSSR and China, where only two and one, respectively, nighttime measurements are available. Therefore, instead of time series of OCET (NOCET), we calculate long-term mean monthly OCET (NOCET) with and without using the moonlight illumination criterion for the whole time period (e.g., from 1948 to 1993 in the contiguous United States). OCET (NOCET) evaluated with the consideration of illumination criterion are named OCET_{*m*} (NOCET_{*m*}). The left-hand panel in Fig. A1 compares the long-term countrywide NOCET and NOCET_{*m*} values. It shows that these two sets of NOCET estimates are consistent. Correlations close to 1 indicate that the application of the illumination criterion does not significantly affect the nighttime NOCET climatology in each of these four regions. The comparison of the long-term OCET and OCET_{*m*} values (Fig. A1), however, indicates that there are some systematic differences. Hahn et al. (1995) have shown that the nighttime average cloud cover is underestimated, and nighttime partly cloudy skies are sometimes ascribed to clear-sky

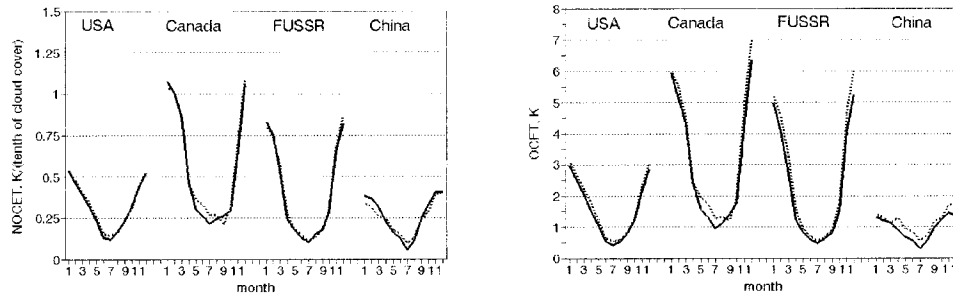


FIG. A1. Comparison of two long-term NOCET and OCET estimates. Solid lines represent standard estimates. Dashed lines represent estimates based only on the data that conform to the moonlight criteria.

conditions. This decreases the estimates of the difference between average and clear-sky cloud cover, ΔCL . But, this also decreases the estimates of difference between air temperatures under average and “clear-sky” conditions, ΔT , because some cloudy events are now wrongly classified as “clear skies.” Because the NOCET estimates are ratios, $\Delta T/\Delta\text{CL}$, we do not see such difference with more accurate NOCET_m values. This is not the case for our OCET estimates; the OCET_m values are systematically (also slightly) higher than the former. The largest bias by absolute value is over the FUSSR in winter (-0.5 K, or -9% of the OCET_m), and the largest bias by percentage is over China in summer (approximately -30% of the OCET_m).

c. Contribution of surface air temperature variations to NOCET changes

Our assessment of the q contribution to the nighttime NOCET (Fig. 2) clearly shows that in a wide range of climate conditions we can parameterize the nighttime NOCET (thus, the longwave-related effects of cloud cover on the surface air temperature, T) with one parameter, specific humidity of the lowest air layer. Of course, the ability of the atmosphere to contain water vapor is strongly dependent on its temperature. Therefore, T makes a large contribution to NOCET by “allowing” q to be high (as well as by intensifying evapotranspiration). Additionally, the warmer the surface, the greater the upward surface outgoing longwave radiation (OLR) will be (Bony et al. 1995; Garratt 1995). This radiation will eventually reach the cloud base (if there is one) and increase its temperature, which in turn will affect the downward longwave flux to the surface from the cloud cover, and thus NOCET.

Here we try to further minimize the radiation effect of T on NOCET hoping that by doing this we can get a better picture of the relationship between NOCET and humidity. This is done by renormalizing the monthly NOCET at each station with a factor $(300/T)^4$, before area-averaging. This renormalized cloud cover–surface air temperature relationship (ROCET), is then compared with the humidity time series, as has been done with NOCET in Fig. 1. This comparison shows that the cor-

relations between ROCET and q_{clear} are generally the same as those between NOCET and q_{clear} during summer and autumn seasons, but are better than the latter during winter and spring seasons over North America and the FUSSR. The joint variance in the ROCET and q_{clear} time series increases by 4%–8% compared to that in NOCET and q_{clear} . In these two seasons, a larger variability of surface temperature in the extratropical land areas, and thus of the surface OLR, somewhat interferes with and reduces the goodness of fit of the NOCET versus q relationship. The variance of annual and interannual variability of surface temperature in warm seasons is low, and therefore, it produces no obvious difference between the NOCET– q and ROCET– q relationships. The use of ROCET instead of NOCET in a parameterization similar to that shown in Eqs. (3.2) and (3.3) increases the joint variance of this parameterization from 83% to 89%.

d. Comparison of the area-averaged NOCET and OCET estimates

We tested the feasibility of using the equation

$$\text{OCET} = \text{NOCET} \times \text{CL} \quad (\text{A.1})$$

to present the area-averaged cloud cover–surface air temperature relationship, OCET [which also can be derived from Eq. (1.1)], with the help of the product of the area-averaged normalized relationship, NOCET, and the area-averaged cloud cover, CL. We needed this equation, because the area-averaged NOCET is much easier to interpret than the OCET; it shows how much surface air temperature change occurs that is associated with a change in one unit of cloud cover in a given month/season/year. When expanding it to any area and time, we assumed that this unit relationship is “similar,” even when the total cloud cover varies widely [i.e., assuming the validity of (A.1)]. Therefore, we can study area-averaged NOCET independently from the cloud cover variations. This strategy has been employed throughout the paper, but beforehand we estimated its performance. We found that the random error of this approximation of the OCET time series with Eq. (A.1) does not exceed 0.1 K, and the correlations between the OCET estimates

from Eq. (A.1) and Eq. (1.1) are extremely high. The biases of this approximation are usually less than 10% of the absolute value of the area-averaged OCET (in the range of [0, 0.3 K]) and are statistically significant at the 0.05 level only over eastern China, where in spring the difference between these two estimates of the OCET reaches 0.3 K.

APPENDIX B

Method of Instrumental Variable

The method of instrumental variable was suggested by Geary (1949) to resolve the problem of estimation of the unknown α parameters in the linear functional relationship

$$Y = \alpha_0 + \alpha_1 X, \quad (\text{B.1})$$

between stochastic variables X and Y , when each of these variables is measured/evaluated with error. The researcher has only “measurements” of Y and X : $\eta = Y + \varepsilon$ and $\xi = X + \delta$. In this situation, if $\sigma_\delta \neq 0$, the least squares method gives biased estimates of the α_1 parameter (Kendall and Stuart 1967). A substitution of measured variables into the functional relationship (B.1) above gives

$$\eta = \alpha_0 + \alpha_1 \xi - \alpha_1 \delta + \varepsilon. \quad (\text{B.2})$$

Geary (1949) suggested using additional information about the X variable that exists in a third “instrumental” variable, ζ , to estimate the unknown α parameters in (B.2). The condition of the use of this variable is that it should be significantly correlated with X but has no correlation with δ and ε :

$$\text{cov}(\delta, \zeta) = 0, \quad \text{cov}(\varepsilon, \zeta) = 0, \quad \text{and} \quad \text{cov}(X, \zeta) \neq 0. \quad (\text{B.3})$$

If these conditions are true (e.g., ζ could be a second independent measurement of X), then a scalar product of ζ and (B.2) will give

$$\begin{aligned} \text{cov}(\eta, \zeta) &= \alpha_0 \text{cov}(1, \zeta) + \alpha_1 \text{cov}(\xi, \zeta) \\ &\quad - \alpha_1 \text{cov}(\delta, \zeta) + \text{cov}(\varepsilon, \zeta) \quad \text{or} \\ \text{cov}(\eta, \zeta) &= \alpha_1 \text{cov}(\xi, \zeta). \end{aligned}$$

Therefore, the ratio $\text{cov}(\eta, \zeta)/\text{cov}(\xi, \zeta)$ gives an asymptotically unbiased estimate of the α_1 parameter, which then is used to estimate the α_0 parameter by the expression

$$\text{avg}(\eta) - \text{avg}(\xi) \text{cov}(\eta, \zeta)/\text{cov}(\xi, \zeta),$$

where “avg” and “cov” are the mean and covariance estimates. This approach was first employed in climatology to estimate the impact of global surface air temperature on regional climate by Vinnikov and Groisman (1979) and then further applied to a climate change detection problem (Vinnikov and Groisman 1982).

REFERENCES

- Angell, J. K., 1990: Variations in the United States cloudiness and sunshine duration between 1950 and the drought year of 1988. *J. Climate*, **3**, 296–308.
- Barkstrom, B. R., 1984: The Earth Radiation Budget Experiment (ERBE). *Bull. Amer. Meteor. Soc.*, **65**, 1170–1185.
- Bony, S., I. P. Duvel, and H. LeTreut, 1995: Observed dependence of the water vapor and clear-sky greenhouse effect on sea surface temperature: Comparison with climate warming experiments. *Climate Dyn.*, **11**, 307–320.
- Brown, R. D., 1997: Historical variability in Northern Hemisphere spring snow covered area. *Ann. Glaciol.*, **25**, 340–346.
- Brunt, D., 1932: Notes on radiation in the atmosphere. *Quart. J. Roy. Meteor. Soc.*, **58**, 389–418.
- Cess, R. D., and Coauthors, 1991: Interpretation of snow–climate feedback as produced by 17 general circulation models. *Science*, **253**, 888–892.
- , and Coauthors, 1996: Cloud feedback in atmospheric general circulation models: An update. *J. Geophys. Res.*, **101**, 12 791–12 794.
- Cubasch, U., J. Waszkewitz, G. Hegerl, and J. Perlwitz, 1995: Climatic changes as simulated in time-slice experiments. *Climatic Change*, **31**, 273–304.
- Dai A., K. E. Trenberth, and T. R. Karl, 1999: Effects of clouds, soil moisture, precipitation and water vapor on diurnal temperature range. *J. Climate*, **12**, 2451–2473.
- Ding, Y.-H., 1994: *Monsoons over China*. Kluwer Academic Publishers, 419 pp.
- Environment Canada, 1995: *The State of Canada's Climate: Monitoring Variability and Change*. Environment Canada, 52 pp.
- Fisk, P. R., 1967: *Stochastically Dependent Equations*. Griffin and Co., 181 pp.
- Fung, I. Y., D. E. Harrison, and A. A. Lacis, 1984: On the variability of the net longwave radiation at the ocean surface. *Rev. Geophys. Space Phys.*, **22**, 177–193.
- Gandin, L. S., and Coauthors, 1976: *Statistical Structure of Meteorological Fields* (in Russian and Hungarian). Az Országos Meteorológiai Szolgálat, 365 pp.
- Garratt, J. R., 1995: Observed screen (air) and GCM surface/screen temperatures: Implications for outgoing longwave fluxes at the surface. *J. Climate*, **8**, 1360–1368.
- Geary, R. C., 1949: Determination of linear relations between systematic parts of variables with errors of observation the variance of which are unknown. *Biometrika*, **17**, 30–59.
- Gosnell, R., C. W. Fairrall, and P. J. Webster, 1995: The sensible heat of rainfall in the tropical oceans. *J. Geophys. Res.*, **100**, 18 437–18 442.
- Groisman, P. Ya., T. R. Karl, and R. W. Knight, 1994a: Observed impact of snow cover on the rise of continental spring temperatures. *Science*, **263**, 198–200.
- , —, and G. L. Stenchikov, 1994b: Changes of snow cover, temperature, and the radiative heat balance over the Northern Hemisphere. *J. Climate*, **7**, 1633–1656.
- , E. L. Genikhovich, and P.-M. Zhai, 1996: “Overall” cloud and snow cover effects on internal climate variables: The use of clear sky climatology. *Bull. Amer. Meteor. Soc.*, **77**, 2055–2065.
- , R. S. Bradley, and B. Sun, 2000: The relationship of cloud cover to near-surface temperature and humidity: Comparison of GCM simulations with empirical data. *J. Climate*, **13**, 1858–1878.
- Hahn, C. J., S. G. Warren, and J. London, 1995: The effect of moonlight on observation of cloud cover at night, and application to cloud climatology. *J. Climate*, **8**, 1429–1446.
- Hansen, J., M. Sato, and R. Ruedy, 1995: Long-term changes of the diurnal temperature cycle; implications about mechanisms of global climate change. *Atmos. Res.*, **37**, 175–210.
- Hartmann, D. L., 1994: *Global Physical Climatology*. Academic Press, 411 pp.

- Henderson-Sellers, A., 1992: Continental cloudiness changes this century. *Geojournal*, **27**, 255–262.
- , and P. J. Robinson, 1986: *Contemporary Climatology*. Longman Scientific and Technical, 439 pp.
- Houghton, J. T., L. G. Meira Filho, B. A. Callander, N. Harris, A. Kattenberg, and K. Maskell, Eds., 1996: *Climate Change 1995: The Science of Climate Change*. Cambridge University Press, 572 pp.
- Houze, R. A., 1993: *Cloud Dynamics*. Academic Press, 576 pp.
- Jones, C., D. E. Waliser, and C. Gautier, 1998: The influence of the Madden-Julian oscillation on ocean surface heat fluxes and sea surface temperature. *J. Climate*, **11**, 1057–1072.
- Jones, P. D., 1994: Hemispheric surface air temperature variations: A reanalysis and an update to 1993. *J. Climate*, **7**, 1794–1802.
- Kaiser, D. P., 1998: Analysis of total cloud amount over China: 1951–1994. *Geophys. Res. Lett.*, **25**, 3599–3602.
- Karl, T. R., and Coauthors, 1993: Asymmetric trends of daily maximum and minimum temperature. *Bull. Amer. Meteor. Soc.*, **74**, 1007–1023.
- Kendall, M. G., and A. Stuart, 1967: *Inference and Relationship*. Vol. 2, *The Advanced Theory of Statistics*, Charles Griffin, 690 pp.
- Kiehl, J. T., 1994: Sensitivity of a GCM climate simulation to differences in continental versus maritime cloud drop size. *J. Geophys. Res.*, **99**, 23 107–23 115.
- Matson, M., and D. R. Wiesnet, 1981: New data base for climate studies. *Nature*, **287**, 451–456.
- Meshcherskaya, A. V., I. G. Belyankina, and M. P. Golod, 1995: Snow depth monitoring in the main corn belt of the former Soviet Union during the period of instrumental observations (in Russian). *Izv. Acad. Sci. USSR, Ser. Geogr.*, **5**, 101–110.
- Mokhov, I. I., and P. K. Love, 1995: Diagnostics of cloudiness evolution in the annual cycle and interannual variability in the AMIP (Cloudiness Diagnostics Subproject 13). *Proc. First Int. AMIP Scientific Conf.*, Monterey, CA, WMO/TD-No. 752, 49–53.
- Norris, J. R., 2000: Interannual and interdecadal variability in the storm track, cloudiness, and sea surface temperature over the summertime North Pacific. *J. Climate*, **13**, 422–430.
- Plantico, M. S., and T. R. Karl, 1990: Is recent climate change across the United States related to rising levels of anthropogenic greenhouse gases? *J. Geophys. Res.*, **95**, 16 617–16 637.
- Robinson, D. A., K. F. Dewey, and R. R. Heim Jr., 1993: Global snow cover monitoring: An update. *Bull. Amer. Meteor. Soc.*, **74**, 1689–1696.
- Ross, R. J., and W. P. Elliott, 1996: Tropospheric water vapor climatology and trends over North America: 1973–1993. *J. Climate*, **9**, 3561–3574.
- Rossow, W. B., and R. A. Schiffer, 1991: ISCCP cloud data products. *Bull. Amer. Meteor. Soc.*, **72**, 2–20.
- Serreze, M., and Coauthors, 2000: Observational evidence of recent changes in the northern high latitude environment. *Climatic Change*, **46**, 159–207.
- Shinoda, T., H. H. Hendon, and J. Glick, 1998: Intraseasonal variability of surface fluxes and sea surface temperature in the tropical western Pacific and Indian Oceans. *J. Climate*, **11**, 1685–1702.
- Stephens, G. L., A. Slingo, M. Webb, and I. Wittmeyer, 1994: Observations of the earth's radiation budget in relation to atmospheric hydrology. Part IV. *J. Geophys. Res.*, **99**, 18 595–18 604.
- Stokes, G. M., and S. E. Schwartz, 1994: The Atmospheric Radiation Measurement (ARM) Program: Programmatic background and design of the cloud and radiation test bed. *Bull. Amer. Meteor. Soc.*, **75**, 1201–1221.
- Sun, B., and P. Ya. Groisman, 1999: Cloud effects on the near surface air temperature: Temporal changes. Preprints, *10th Symp. on Global Change Studies*, Dallas, TX, Amer. Meteor. Soc., 277–281.
- , and —, 2000: Cloudiness variations over the former Soviet Union. *Int. J. Climatol.*, **20**, 1097–1111.
- Thiessen, A. H., 1911: Precipitation averages for large areas. *Mon. Wea. Rev.*, **39**, 1082–1084.
- Vinnikov, K. Ya., and P. Ya. Groisman, 1979: An empirical model of the present-day climatic changes (in Russian). *Meteor. Hydrol.*, No. 3, 25–36.
- , and —, 1982: Empirical study of climate sensitivity. *Phys. Atmos. Oceans*, **18**, 1159–1169.
- , —, and K. M. Lugina, 1990: The empirical data on modern global climate changes (temperature and precipitation). *J. Climate*, **3**, 662–677.
- Warren, S. G., and W. J. Wiscombe, 1980: A model for spectral albedo of snow. II: Snow containing atmospheric aerosols. *J. Atmos. Sci.*, **37**, 2734–2745.
- Weare, B. C., 1994: Interrelationships between cloud properties and sea surface temperatures on seasonal and interannual time scales. *J. Climate*, **7**, 248–260.
- , and AMIP Modeling Groups, 1996: Evaluation of the vertical structure of zonally averaged cloudiness and its variability in the Atmospheric Model Intercomparison Project. *J. Climate*, **9**, 3419–3431.
- Weaver, C. P., and V. Ramanathan, 1997: Relationships between large-scale vertical velocity, static stability, and cloud radiative forcing over Northern Hemisphere extratropical oceans. *J. Climate*, **10**, 2871–2887.
- Wielicki, B. A., R. D. Cess, M. D. King, D. A. Randall, and E. F. Harrison, 1995: Mission to Planet Earth: Role of clouds and radiation in climate. *Bull. Amer. Meteor. Soc.*, **76**, 2125–2153.
- Zhai, P.-M., and R. E. Eskridge, 1997: Atmospheric water vapor over China. *J. Climate*, **10**, 2643–2652.
- Zhang, Y.-C., W. B. Rossow, and A. A. Lacis, 1995: Calculation of surface and top of atmosphere radiation fluxes from physical quantities based on ISCCP data sets. Part I: Methods and sensitivity to input data uncertainties. *J. Geophys. Res.*, **100**, 1149–1165.